

Atomic Layer Deposition and Chemical Vapor Deposition Precursor Selection Method Application to Strontium and Barium Precursors

Timothy P. Holme* and Fritz B. Prinz

Mechanical Engineering Department, Stanford University, 440 Escondido Mall Stanford, California 94305

Received: April 26, 2006; In Final Form: May 23, 2007

A new selection method for atomic layer deposition (ALD) or chemical vapor deposition (CVD) precursors is proposed and tested. Density functional theory was used to simulate Sr and Ba precursors, and several precursors were selected and used to grow films via ALD as test cases for the precursor selection method. The precursors studied were $M(x)_2$ ($M = \text{Sr}, \text{Ba}$; $x =$ tetramethylheptanedionate (tmhd), acetylacetonate (acac), hexafluoroacetylacetonate (hfac), cyclopentadienyl (H_5C_5), pentamethylcyclopentadienyl (Me_5C_5), *n*-propyltetramethylcyclopentadienyl (PrMe_4C_5), tris(isopropylcyclopentadienyl) ($\text{Pr}^i_3\text{H}_2\text{C}_5$), tris(isopropylcyclopentadienyl)(THF) ($\text{Pr}^i_3\text{H}_2\text{C}_5$)(OC_4H_8), tris(isopropylcyclopentadienyl)(THF)₂ ($\text{Pr}^i_3\text{H}_2\text{C}_5$)(OC_4H_8)₂, tris(*tert*-butylcyclopentadienyl) ($\text{Bu}^t_3\text{H}_2\text{C}_5$), tris(*tert*-butylcyclopentadienyl)(THF) ($\text{Bu}^t_3\text{H}_2\text{C}_5$)(OC_4H_8), heptafluoro-2,2-dimethyl-3,5-octanedionate (fod)). The energy required to break bonds between the metal atom and the ligands was calculated to find which precursors react most readily. In the case of tmhd and Cp precursors, the energy required to break bonds in the precursor ligand was studied to evaluate the most likely mechanism of carbon incorporation into the film. Trends for Ba and Sr followed each other closely, reflecting the similar chemistry among alkaline earth metals. The diketonate precursors have stronger bonds to the metals than the Cp precursors, but weaker bonds within the ligand, explaining the carbon contamination found in experimentally grown films. Atomic layer deposition of SrO was tested with $\text{Sr}(\text{tmhd})_2$ and $\text{Sr}(\text{PrMe}_4\text{Cp})_2$ and oxygen, ozone, and water as oxygen sources. No deposition was measured with tmhd precursors, and SrO films were deposited with PrMe_4Cp with a source temperature of 200 °C and at substrate temperatures between 250 and 350 °C with growth rates increasing for oxygen sources in this order: $\text{O}_2 < \text{H}_2\text{O} < \text{O}_2 + \text{H}_2\text{O}$. The experimental results support the predictions based upon calculations: PrMe_4Cp and Me_5Cp precursors are expected to be the best precursors among those studied for Ba and Sr film growth.

1. Introduction

Interest in atomic layer deposition (ALD) or chemical vapor deposition (CVD) fabrication of thin films of Ba- and Sr-containing oxides is driven by several applications: insulators such as $(\text{Ba},\text{Sr})\text{TiO}_3$ for dynamic random access memories,¹ ferroelectrics such as SrTiO_3 , $\text{SrBi}_2\text{Ta}_2\text{O}_9$, and $\text{SrBi}_2\text{Nb}_2\text{O}_9$ for computer memory,² high- T_c superconductors such as $\text{YBa}_2\text{Cu}_3\text{O}_{7-x}$ and $\text{Bi}_2\text{Sr}_2\text{CaCu}_2\text{O}_{8+\delta}$,³ electroluminescent films such as $\text{SrS}:\text{Ce}$,⁴ ionic conductors such as BaZrO_3 for fuel cell electrolytes,⁵ and mixed-electronic ionic conductors such as $(\text{La}_x\text{Sr}_{1-x})\text{MnO}_3$, $(\text{La}_x\text{Sr}_{1-x})\text{CoO}_3$ for fuel cell cathodes.⁶

The most commonly used Sr precursor cited in literature is the β -diketonate precursor $\text{Sr}(\text{tmhd})_2$ (tmhd = 2,2,6,6-tetramethyl-3,5-heptanedione) (also referred to as dipivaloylmethane or DPM). Atomic layer deposition (ALD) of Sr with tmhd precursors often leads to films with significant carbon contamination or formation of the SrCO_3 phase.⁷ Cyclopentadienyl (Cp) precursors and their derivatives have been more successful in deposition of Sr films,⁸ and carbon contamination levels were very low (<0.3 at %).⁹ According to a study by Hatanpää, the most thermally stable and volatile Ba precursors are Cp precursors with *tert*-Butyl and isopropyl ligands.¹⁰

Hinds reports that the vapor pressure stability of $\text{Ba}(\text{tmhd})_2$ is low at typical growth temperatures.¹¹ Momose et al. find that

Sr and $\text{Ba}(\text{tmhd})_2$ precursors decompose in the gas phase at substrate temperatures 300 °C, whereas Sr or Ba atoms are incorporated into films at substrate temperatures of ≥ 400 °C.¹² Precursor thermal decomposition suggests that the precursor will not be suited to ALD, as self-limiting reaction cannot be achieved.

The object of this study is to present a method by which precursors may be tested computationally for their suitability for ALD processes. Computational screening may provide a much faster test of a precursor than experimental use. In addition, it may provide insight into the design of an optimal precursor. As a test case, the method will be used to determine which Ba and Sr precursors have optimal properties for ALD deposition and to examine the mechanism of carbon contamination with β -diketonates. Primary focus is on β -diketonate and Cp compounds. The Cp compounds selected for study include: cyclopentadienyl (Cp), pentamethylcyclopentadienyl (Me_5Cp), *n*-propyltetramethylcyclopentadienyl (PrMe_4Cp), tris(isopropylcyclopentadienyl) ($\text{Pr}^i_3\text{H}_2\text{Cp}$), tris(isopropylcyclopentadienyl)(THF) ($\text{Pr}^i_3\text{H}_2\text{Cp}$)(OC_4H_8), tris(isopropylcyclopentadienyl)(THF)₂ ($\text{Pr}^i_3\text{H}_2\text{Cp}$)(OC_4H_8)₂, tris(*tert*-butylcyclopentadienyl) ($\text{Bu}^t_3\text{H}_2\text{Cp}$), and tris(*tert*-butylcyclopentadienyl)(THF) ($\text{Bu}^t_3\text{H}_2\text{Cp}$)(OC_4H_8). The β -diketonate parent compounds, acetylacetonates (acac), are also studied. To increase precursor volatility, often the ligands are fluorinated,¹³ so $\text{Sr}(\text{fod})_2$ and $\text{Sr}(\text{hfac})_2$ (fod = 6,6,7,7,8,8,8-heptafluoro-2,2-dimethyl-3,5-octanedionate, hfac = hexafluoroacetylacetonate) are studied.

* Corresponding author. E-mail: tholme@stanford.edu.

As the reaction mechanism for these precursors is unknown, this study evaluates the starting and ending points of the reaction to compare thermodynamic driving forces for breaking various bonds in the precursor. By comparing the energy required for bond breaking among different precursors, we will make a prediction about which precursors have favorable driving forces for reaction.

2. Experimental Details

2.1. Details of Calculations. The Los Alamos basis set LANL2DZ (effective core potential and a double- ζ valence shell¹⁴) was used for Sr and Ba; for all other atoms the basis set used was 3-21G or 6-311G as described below. Both Hartree–Fock (HF) and Becke’s generalized gradient approximation¹⁵ with the Lee–Yang–Parr correlation functional¹⁶ (B3LYP) were used for calculations. The geometry of each molecule was optimized at the HF/3-21G+LANL2DZ level and subsequently refined at the B3LYP/6-311G+LANL2DZ level. B3LYP/LANL2DZ has previously been applied to studying ALD reactions.¹⁷ All reported energies are found at the B3LYP/6-311G+LANL2DZ level. Gaussian ‘03 was used for all calculations.

To calculate the bond energy of compound AB, the following formula was used

$$E = E_A + E_B - E_{AB} \quad (1)$$

where E_{AB} is the energy of the compound and $E_{A,B}$ are the energies of the constituents A and B, each after their geometry has been optimized. In this definition, the energy required to break a bond between two constituents is positive (requires energy input).

2.2. Details of ALD Process. ALD of SrO films was performed on Si(100) substrates in a commercial reactor (Cambridge Nanotech Savannah 200) with Sr(PrMe_4Cp)₂·dimethoxyethane (Alfa Aesar J27Q052) and Sr(tmhd)₂ (Strem B1950041). The oxygen sources were oxygen (Praxair 99.993%), ozone (ozone generator MKS AX8560), and deionized water.

The source temperature was varied from 50 to 200 °C; the substrate temperature was varied from 150 to 350 °C. The lines and valves leading from the source to the reactor were heated to a temperature between the source and substrate temperature, as were the reactor walls. Typical ozone or oxygen pulse times were 4 s, typical water pulse times were 0.5 s, and typical precursor pulse times were 0.2 s. The purge time between pulses was 10–15 s. An oxygen flow rate of 0.5 slm was maintained by a mass flow controller.

Films were characterized by ellipsometry, X-ray photoemission spectroscopy (XPS), X-ray diffraction (XRD), and scanning electron microscopy (SEM). Samples were exposed to air for a short time between growth and transfer to the XPS vacuum chamber; thus some reaction between the as-grown film and air cannot be ruled out. Depth profiling with XPS was done by sputtering with Ar ions at 3 kV, 10 mA, and 1×10^{-7} Torr, giving a sputtering rate of approximately 1 Å/s.

3. Results

3.1. Calculation Results. The optimized geometry of each ligand is shown in Figure 1.

Table 1 shows the energy required to break the bonds in the precursor molecule between the first ligand and the M–ligand complex and between the second ligand and the M atom. For a facile ALD reaction, it is desirable to have the ligand weakly bound to the metal. It can be seen that the Cp compounds have

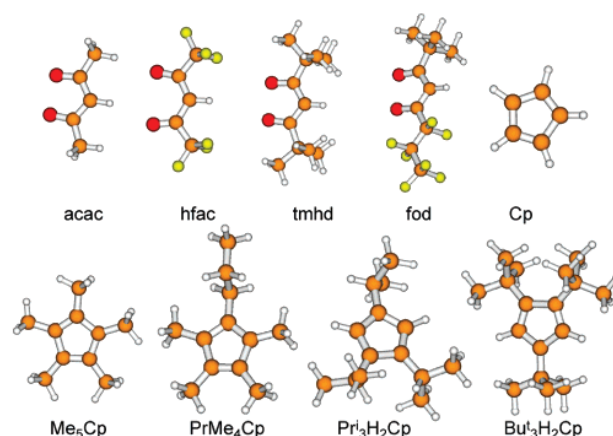


Figure 1. Optimized structures of each ligand. Carbon atoms shown in brown, hydrogen in white, oxygen in red, and fluorine in yellow.

TABLE 1: Energy (eV) Required to Break Bonds between the First and Second Ligand and Sr and Ba for Each Precursor Studied

precursor	first ligand	second ligand
Sr(acac) ₂	4.99	3.79
Sr(hfac) ₂	5.45	4.33
Sr(tmhd) ₂	4.94	3.75
Sr(fod) ₂	5.38	4.18
Sr(Cp) ₂	3.10	1.88
Sr(Me ₅ Cp) ₂	2.42	1.24
Sr(PrMe ₄ Cp) ₂	2.43	1.24
Sr(Pr ₃ H ₂ Cp) ₂	2.58	1.40
Sr(Bu ₃ H ₂ Cp) ₂	2.54	1.38
Ba(acac) ₂	4.85	3.88
Ba(hfac) ₂	5.42	4.50
Ba(tmhd) ₂	4.80	3.84
Ba(fod) ₂	5.30	4.31
Ba(Cp) ₂	3.10	2.03
Ba(Me ₅ Cp) ₂	2.38	1.38
Ba(PrMe ₄ Cp) ₂	2.40	1.40
Ba(Pr ₃ H ₂ Cp) ₂	2.59	1.56
Ba(Pr ₃ H ₂ Cp) ₂ (THF)	2.59	1.86
Ba(Pr ₃ H ₂ Cp) ₂ (THF) ₂	2.57	2.18
Ba(Bu ₃ H ₂ Cp) ₂	2.61	1.54
Ba(Bu ₃ H ₂ C ₅) ₂ (THF)	2.71	1.83

weaker bonds to M than the β -diketonates, and that the first ligand is bound more tightly to M than the second ligand. Fluorinated compounds are bound more tightly than unfluorinated relatives. The bonds between Cp rings and M weaken when methyl groups are substituted for hydrogen in the ring, but the chemistry is relatively unchanged when a propyl group is substituted for a methyl group. The trends between Ba and Sr are well matched, with the first ligand being slightly more strongly bonded to Sr, and the second ligand has a slightly stronger bond to Ba. As Momose¹² finds, the Ba–O bond is longer than the Sr–O bond in the tmhd precursor (2.60 Å compared to 2.43 Å from these calculations), so the Sr–O bond is stronger than the Ba–O bond.

To investigate the most likely sources for carbon contamination in Sr films grown with diketonate precursors noted by Kosola,⁷ various bonds in the tmhd ligand were broken. The results are illustrated in Figure 2. The bonds within the ligand are weaker than the bond between the ligand and the M atom, so it is likely that the ligand thermally decomposes before incorporation into the film, in agreement with experiment.¹² As Nakamura finds, diketonate precursors tend to decompose and leave carbon contamination in the film at lower temperatures than the temperatures for onset of rapid film growth.¹⁸ The

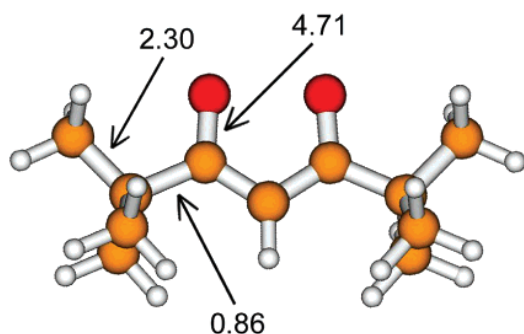


Figure 2. Energy (eV) required to break bonds within a single tmhd ligand. For comparison, the ligand is bound to the Sr atom by 3.75 eV.

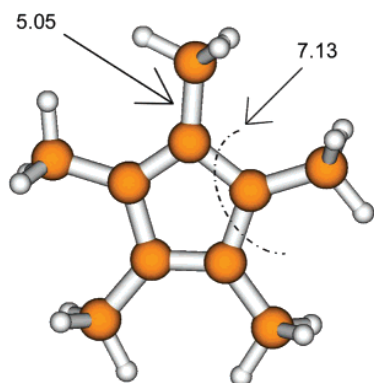


Figure 3. Energy (eV) required to break bonds within a single Me₅-Cp ligand.

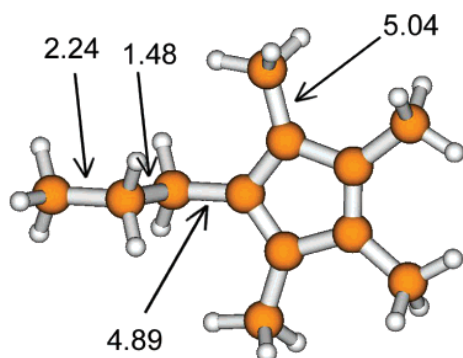


Figure 4. Energy (eV) required to break bonds within a single PrMe₄-Cp ligand.

weakest bond is between the C(CH₃)₃ group and the rest of the ligand, suggesting that it is the most likely bond to decompose.

For comparison, the energy required to break bonds in Me₅-Cp and PrMe₄Cp are investigated. The energy required to break bonds in Me₅Cp is shown in Figure 3. In Me₅Cp, to remove a methyl group from the ring costs 5.05 eV, and to remove a CCH₃ group from the ring requires 7.13 eV. Both of these are larger than the energy required to break bonds in tmhd precursors, showing that the Me₅Cp ligand is more stable and less likely to cause carbon contamination in the film.

The energy to break bonds in the PrMe₄Cp ligand is shown in Figure 4. The energy cost to break a bond between the ring and a methyl group is equal to that in the Me₅Cp ligand to within the accuracy of the calculation. The weak bond in the ligand is between the ethyl CH₃CH₂ group. This bond is more stable than the weakest bond in the tmhd ligand. Therefore the Cp precursors are expected to decompose less readily than the tmhd precursor.

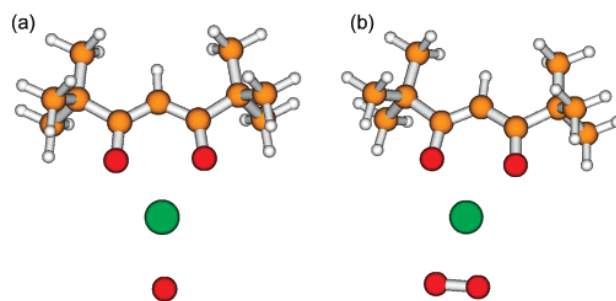


Figure 5. Stable geometry of Sr bonded to one tmhd ligand and one (a) or two (b) oxygen atoms from the second tmhd ligand. Sr atom shown in green.

TABLE 2: Comparison between Experimental Crystal Structure and Simulated Geometry for Ba(Bu^tH₂Cs)₂ (THF)

	experiment	simulation
Ba–C(ring) (mean) (Å)	3.017	3.136
Ba–centroid (mean) (Å)	2.768	2.890
Ba–O (Å)	2.743	2.800
centroid–Ba–centroid (deg)	148.1	151.5

To verify that the Sr–O bonds in the tmhd precursor are broken rather than the O–C bonds, the bond strength of each bond was calculated. For Sr bonded to one tmhd ligand and one or two oxygen atoms (structure shown in Figure 5 (a) and (b) respectively), the energy to remove the remainder of the second ligand is 6.75 and 10.17 eV, respectively. Because these energy barriers are quite large, we expect the entire ligand to be removed from the Sr atom. Indeed, an isotopic exchange experiment shows that the majority of the oxygen atoms in the resulting film come from the gas phase rather than the ligand.¹⁹

The authors know of no amino Sr or Ba precursor, but simulated one, Sr(N(CH₃)₂)₂. The precursor was unstable, with a negative bond energy and very long Sr–N bonds. This reflects that the amino–Sr molecule is unstable, which coheres with the apparent difficulty in synthesis of an amino–Sr molecule.

Ba precursors including a THF ligand were included in the above calculations for comparison to Hatanpää's results.¹⁰ The presence of THF does not have a significant impact on the bond energy between Ba and the ligand. THF was found to be much more weakly bound to Ba than the ligands (bond energies falling in the range 0.5–0.7 eV); thus the THF is expected to readily detach from the precursor at elevated reaction temperatures and the precursor should behave as the precursor without THF. The geometry of the simulated precursor is very close to the experimental crystal structure.¹⁰ A comparison of key bond lengths and angles is presented in Table 2. Aside from the consistent overestimate of bond lengths endemic to DFT methods (here 2–4%), the results are in close agreement with the experimental crystal structure.

3.2. ALD Results. In the wide range of source temperatures, substrate temperatures, and oxidants investigated, SrO was not successfully grown with the Sr(tmhd)₂ precursor in this study, despite reports from other groups of successful growth.^{7,20} It is to be noted that Niinisto observed growth of SrCO₃ rather than SrO due to use of ozone as oxidant.⁷

Growth of SrO with Sr(PrMe₄Cp)₂ was observed in an ALD window of 250–350 °C and source temperatures 190–200 °C with oxygen and water as oxidants. Growth rates with oxygen were approximately 0.07 Å/cycle, independent of substrate temperature within the ALD window. Growth rates with water were approximately 0.2 Å/cycle, also independent of substrate temperature in the window. Depth profiling with XPS showed

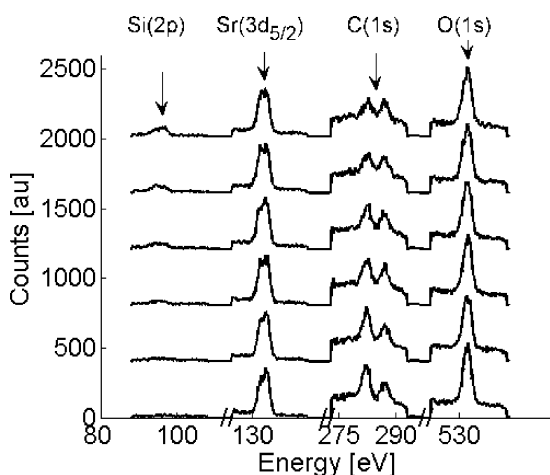


Figure 6. XPS depth profile of SrO grown on a Si substrate with water and $\text{Sr}(\text{PrMe}_4\text{Cp})_2$. Si signal due to substrate. Measurements after 2 nm sputtering are offset along the y-axis for clarity. Note broken x-axis.

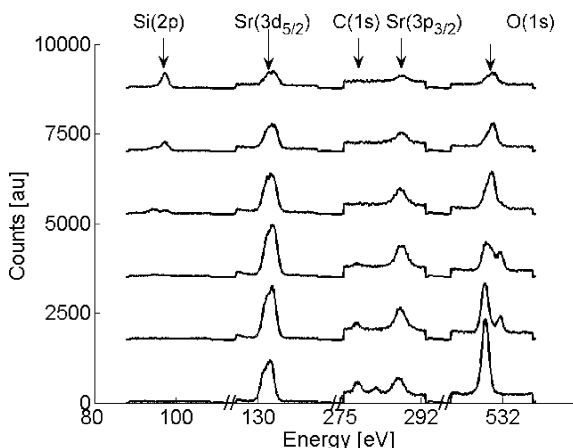


Figure 7. XPS depth profile of SrO grown on a Si substrate with water, oxygen, and $\text{Sr}(\text{PrMe}_4\text{Cp})_2$. Si signal from substrate. Measurements after 1 nm material sputtered away are offset along the y-axis for clarity. Note broken x-axis.

C contamination throughout the film grown with water, shown in Figure 6. Growth with pulses of both water and oxygen between Sr precursor pulses was tested. Using both oxygen and water, films grew at growth rates of 0.4 Å/cycle. Carbon contamination in the bulk was diminished, as shown by the XPS depth profile in Figure 7.

4. Discussion

An ideal precursor has a relatively weak bond between the metal atom and the ligand. To further weaken the bond between M and the ligand, the ligand should donate charge to antibonding orbitals between M and the ligand. When substituted for methyl groups in β -diketonates, the strongly electronegative F draws charge density toward itself, removing charge from antibonding orbitals, and strengthening the M–ligand bond. Therefore, fluorinated precursors sacrifice ease of reaction, and therefore growth rate, for greater volatility. Further, some have noted F contamination in films grown with hfac precursors.²¹ Therefore, it is hypothesized that hfac and fod are not preferred precursors for Sr and Ba film growth. The strong tmhd–Sr bonds explain why reaction with water or oxygen does not occur at temperatures below their thermal decomposition temperature,⁸ and

therefore require the much more reactive ozone to be used as the oxygen source.

Cyclopentadienyl precursors have much weaker bonds to Sr and Ba than β -diketonates. When electron donating methyl groups are substituted for hydrogen on the Cp ring, the bond is further weakened. It seems that substituting longer carbon chains for methyl groups does not greatly affect the bond strength between M and the ligand.

The weakest bond in tmhd precursors is that between the $\text{C}(\text{CH}_3)_3$ end group and the rest of the ligand. This group is less weakly bound than the metal atom, thus this bond is the most likely site for reaction or decomposition. If the $\text{C}(\text{CH}_3)_3$ group is broken, the radical could react with Sr–O bonds in the growing film, thus describing a likely route for carbon incorporation into the film. If the group reacts with ozone in the gas phase, it may be further broken down or passivated.

In situ studies to elucidate the mechanism of reaction are necessary to perform more complete analysis of the reaction kinetics of Sr and Ba precursors and oxide growth by ALD.

5. Conclusions

A method was presented to computationally screen precursors for suitability in ALD processes. A quantum chemical study of the precursor reaction thermochemistry proves to be a good predictor of ease of use in ALD growth. The results of the method agree with experience gained from years experimentation with precursor and oxidant selection, suggesting the utility of the computational screening method.

Fluorine containing precursors, though they have higher vapor pressures, are not desirable because strong ligand–M bonds result in low growth rates and weak bonds in the ligand result in probable F contamination in the grown films. Diketonates have stronger bonds to metal atoms than cyclopentadienyl rings and weaker bonds within the ligand, suggesting that diketonate precursors will have lower growth rates and more likely carbon contamination in the film.

Experimental observations of C and F contamination in films grown with diketonate precursors are explained by the weak bonds within the ligand. Isotope exchange experiments showing that O content in the film comes from the gas phase rather than the ligand are supported by our finding that the Sr–O bond is weaker than the O–C bond in the diketonate ligand.

ALD growth of SrO with diketonate precursors was not successful in this study, though deposition has been reported in previous studies. Deposition with the Me_5Cp precursor has been accomplished at reasonable temperatures of sublimation with growth rates of 0.4 Å/cycle and low carbon contamination in the bulk. Growth rates with different oxygen sources increased in the order $\text{O}_2 < \text{H}_2\text{O} < \text{O}_2 + \text{H}_2\text{O}$.

On the basis of the preceding bond strength analysis and available experimental evidence, the PrMe_4Cp and Me_5Cp precursors appear to be the best precursors for Sr and Ba film growth via ALD or CVD.

Acknowledgment. The authors would like to thank Swagelok for providing high temperature ALD values.

References and Notes

- (1) Ezhilvalavan, S.; Tseng, T. Y. *Mater. Chem. Phys.* **2000**, *65*, 227–248.
- (2) Jones, A. C.; Chalker, P. R. *J. Phys. D* **2003**, *36*, R80–95.
- (3) Shen, Z. X.; Dessau, D. S. *Phys. Rep.* **1995**, *253*, 1–162.
- (4) Heikkinen, H.; Johansson, L. S.; Nykanen, E.; Niinisto, L. *Appl. Surf. Sci.* **1998**, *133*, 205–12.
- (5) Kreuer, K. D. *Annu. Rev. Mater. Res.* **2003**, *33*, 333–359.

- (6) Mogensen, M.; Skaarup, S. *Solid State Ion. Diffus. React.* **1996**, 86–88, 1151–60.
- (7) Kosola, A.; Putkonen, M.; Johansson, L.; Niinisto, L. *Appl. Surf. Sci.* **2003**, 211, 102–12.
- (8) Vehkamäki, M.; Hatanpää, T.; Hanninen, T.; Ritala, M.; Leskelä, M. *Electrochem. Solid-State Lett.* **1999**, 2, 504–6.
- (9) Putkonen, M. Ph.D. thesis, Helsinki University of Technology, Espoo, Finland, 2002.
- (10) Hatanpää, T.; Vehkamäki, M.; Mutikainen, I.; Kansikas, J.; Ritala, M.; Leskelä, M. *Dalton Trans.* **2004**, 8, 1181–8.
- (11) Hinds, B. J.; McNeely, R. J.; Studebaker, D. B.; Marks, T. J.; Hogan, T. P.; Schindler, J. L.; Kannewurf, C. R.; Zhang, X. F.; Miller, D. *J. J. Mater. Res.* **1997**, 12, 1214–36.
- (12) Momose, S.; Nakamura, T.; Tachibana, K. *Jpn. J. Appl. Phys. Suppl.* **2000**, 39, 5384–8.
- (13) Fahlman, B. D.; Barron, A. R. *Adv. Mater. Opt. Electron.* **2000**, 10, 223–232.
- (14) Wadt, W. R.; Hay, P. J. *J. Chem. Phys.* **1985**, 82, 284–298.
- (15) Becke, A. D. *Phys. Rev. A* **1988**, 38, 3098–3100.
- (16) Lee, C. T.; Yang, W. T.; Parr, R. G. *Phys. Rev. B* **1988**, 37, 785–789.
- (17) Han, J. H.; Gao, G.; Widjaja, Y.; Garfunkel, E.; Musgrave, C. B. *Surf. Sci.* **2004**, 550, 199–212.
- (18) Nakamura, T.; Tai, R.; Nishimura, T.; Tachibana, K. *J. Electrochem. Soc.* **2005**, 152, C584–7.
- (19) Nakamura, T.; Momose, S.; Tachibana, K. *Jpn. J. Appl. Phys.* **2001**, 40, 6619–22.
- (20) Aarik, J.; Aidla, A.; Jaek, A.; Leskela, M.; Niinisto, L. *J. Mater. Chem.* **1994**, 4, 1239–1244.
- (21) Bedoya, C.; Condorelli, G. G.; Di Mauro, A.; Anastasi, G.; Fragala, I. L.; Lisoni, J. G.; Wouters, D. *Mater. Sci. Eng. B* **2005**, 118, 264–9.